# Chapter 9 RF Exposure

## Overview

This chapter contains information as to how the product was determined to be compliant with FCC Part 24 subsection 24.51

## Contents

9.1 RF Human Exposure - FDTD Analysis and SAR Testing . . . . . 9-2
9.2 Summary and Conclusions . . . . . 9-4
9.3 Computer Hardware and Software Used for Performing Calculations . 9-4
9.4 2 FDTD Models . . . . . 9-5
9.5 FDTD Calculation and Measurements of SAR in Kuster Head and Shoulders Homogeneous Model . . . . . 9-14
9.6 FDTD Calculation of SAR in REMCOM Head and Shoulders Inhomogeneous Model (no radome attached). . . . . 9-23

## 9.1 RF Human Exposure - FDTD Analysis and SAR Testing

### 9.1.1 Applicable FCC Rules

FCC Subpart 24.51 - Applications for Type Approval of transmitters operating within the PCS region must determine that the equipment complies with IEEE C95.1-1991, “IEEE Standards for Safety Levels with Respect to Human Exposure to Radio Frequency Electromagnetic Fields, 3 kHz to 300 GHz” as measured using methods specified in IEEE C95.3 - 1991, “Recommended Practice for the Measurement of Potentially Hazardous Electromagnetic Fields - RF and Microwave.”

### 9.1.2 Test Configuration

RF human exposure configurations were setup, tested, and evaluated by the following independent laboratories for the original Remote Unit. The R3 WCS is a revision of the original PCS version and utilizes the same enclosures with a WCS revised antenna. Modifications were made to the antenna for utilization within the WCS spectrum, therefore, additional modelling was completed by Dr. William Guy. Due to the accuracy of correlation from the modelling to the SAR testing, AT&T feels that modelling of this product revision is adequate.

#### 9.1.2.1 Modelling

Modelling was performed on both Remote Units R1, R3 PCS, and R3 WCS by Bioelectromagnetics Consulting, 18122 60th Pl. N.E., Kenmore, Washington 98028, with Dr. William Guy as primary consultant, responsible for carrying out the FDTD numerical analysis of the near fields, far fields, and SAR distributions from the R3 WCS Outdoor Unit. As primary consultant, additional responsibilities included the evaluation and analysis of the SAR data from the independent SAR measurement laboratories utilized during SAR measurements of the R1.

#### 9.1.2.2 SAR Testing

SAR testing performed on the original R1 Remote Unit and correlated to the models by SAR testing Schmid & Partner Engineering AG (SPEAG), Staffelstrasse 8, 8045 Zurich, Switzerland, with Dr. Neils Kuster as the project director, who was responsible for carrying out measurements of the near and far fields for the R1 Outdoor Unit and

SAR distribution in homogeneous phantom head and a flat rectangular tissue models exposed to the antenna fields.

SARTest Ltd., Oakfield Laboratories, Cudworth Lane, Newdigate, Surrey RH5 5DR. UK., with M.I. Manning as project director, who was responsible for carrying out measurements of the near and far fields for the R1 Outdoor Unit and SAR distribution in a heterogeneous phantom head model and a flat heterogeneous rectangular tissue model exposed to the antenna fields.

### 9.1.3 Test Results

Bioelectromagnetics Consulting completed the FDTD measurements on the R3 WCS Cushcraft antenna, and found the product to be compliant with FCC Subpart 27.52 as it relates to WCS spectrum.

The results of the SAR calculations are summarized in Table 9.1.

*Table 9.1 Summary and Comparison of Calculated and Measured Maximum SARs to FCC MPL for Various Tissue Models Exposed to AT&T R3 WCS Cushcraft Antenna.*

| Model | Peak SAR (W/kg) e.i.r.p. = 4.0 W | 1 Gram Avg. SAR (W/kg) e.i.r.p. = 4.0 W | dB from FCC MPL | | |
|---|---|---|---|---|---|
| | | | e.i.r.p. = 2.0 W | e.i.r.p. = 3.0 W | e.i.r.p. = 4.0 W |
| SPEAG Head, nose over array | 1.11 | 0.570 | -7.48 | -5.73 | -4.48 |
| SPEAG Head, nose over patch 1 | 1.73 | 0.878 | -5.61 | -3.86 | -2.61 |
| SPEAG Head, nose over patch 1 with radome | 1.12 | 0.721 | -6.46 | -4.71 | -3.46 |
| SPEAG Head, nose over patch 2 | 0.883 | 0.507 | -6.17 | -4.42 | -3.17 |
| SPEAG Head, nose over patch 4 | 1.05 | 0.631 | -7.04 | -5.29 | -4.04 |
| REMCOM Head, nose over patch 1 | 2.39 | 0.715 | -7.47 | -5.72 | -4.47 |

## 9.2 Summary and Conclusions

The FDTD method was used to calculate the far field antenna patterns and near electric and magnetic fields for the AT&T Cushcraft 2.357 GHz antenna radiating in free space for an input power of 158.5 mW split evenly between two coaxial antenna input feeds. The antenna patterns and gain closely agreed with the antenna manufacturer's measured values. The SPEAG (Schmid & Partner, Engineering AG (SPEAG), Staffelstrasse 8, 8045 Zurich, Switzerland) homogeneous head model (Kuster head model) and the REMCOM inhomogeneous head model used in the previous AT&T RU Antenna study as reported in January 12, 1999 were also used in this study.

The finite difference time domain (FDTD) technique was used to calculate the near and far fields and induced SAR patterns in exposed tissues from the antenna. The FDTD technique is currently the most popular theoretical method of choice for analyzing the safety and compliance of wireless technology devices with human RF exposure MPLs.

## 9.3 Computer Hardware and Software Used for Performing Calculations

### 9.3.1 Computer Hardware

The theoretical calculations were performed on a dual Pentium 500 MHz, home built PC Workstation equipped with a SuperMicro P6DGU motherboard containing 2.0 Gbyte of RAM and 80 Gbytes of hard disk space operating under Windows 2000 Server Operating System.

### 9.3.2 Computer Software

An FDTD software package commercially available from REMCOM Corporation [State College, PA], called XFDTD (version 505) was used to carry out all of the SAR calculations at a frequency of 2357.0 MHz discussed in this report. All of the calculations of SAR conducted with the XFDTD software utilized the default timestep interval of 1.926 ps and total of 4000 time steps. The XFDTD software calculates the SAR based on the 3 electric field components corresponding to the 3 edges

intersecting at the corner nearest the origin of each FDTD cell. A feature of the new software allows the conversion of the model, field and SAR distribution images from the workstation monitor screen into BMP files for storage or transfer to other imaging software.

The antenna was completely disassembled and the dimensions of each part were carefully measured with Fowler Ultra-Cal model III digital calipers. The outline of each antenna aluminum sheet was traced on a 11x17-inch sheet of mm scale graphics paper. The coordinates of the outside periphery of the antenna ground plane and the polygonal shaped patch array and associated stripline circuitry entered manually to the XFDTD program through its graphical users interface (GUI).

The GUI feature of the XFDTD program was then used to assemble and convert the antenna ground plane and patch array/stripline outlines into solid 1mm thick sheet metal solid objects within a 285x306x342, cell mesh of 1x1x1-mm cubical cells. The objects were graphically reassembled and the other antenna parts, including feed points were added via the GUI and a 1 volt, zero phase source in series with a 50 ohm resistance was applied at the lower feed point and a similar source with an increase of 20 degrees in phase was applied at the upper feed point. All data and graphs resulting from the calculations were calibrated to correspond to an a total input power of 0.1585 watts or 22 dBm. This results in an effective radiated power (e.i.r.p.) of 4 watts from the 14 dB gain antenna.

## 9.4 2 FDTD Models

### 9.4.1 Antenna Model

Figure 9.1 illustrates a graph of the 276x311 mm antenna ground plane in the y-z plane of the mesh.

*Figure 9.1*

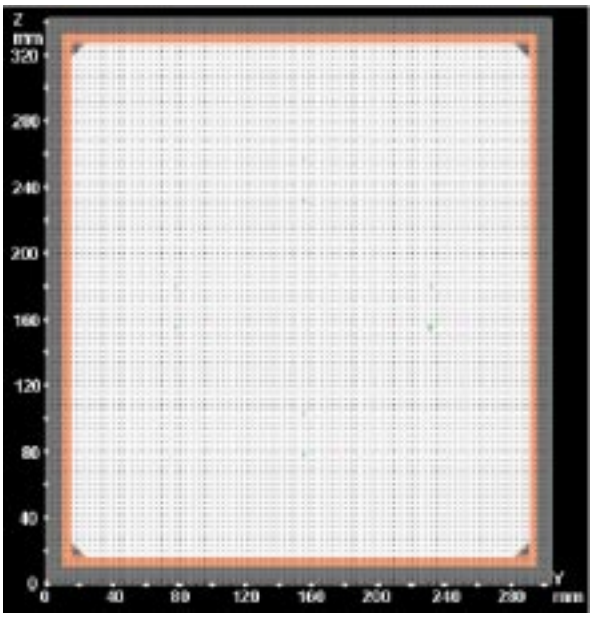


Figure 9.2 illustrates a graph of the stripline circuitry and associated connected square patches in the yz plane and Figure 9.3 illustrates a graph of the upper square patches and mounting screws.

*Figure 9.2*

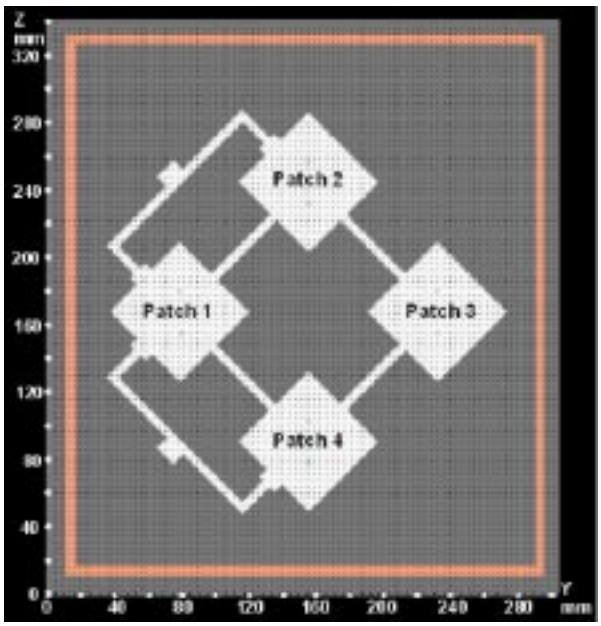

*Figure 9.3*

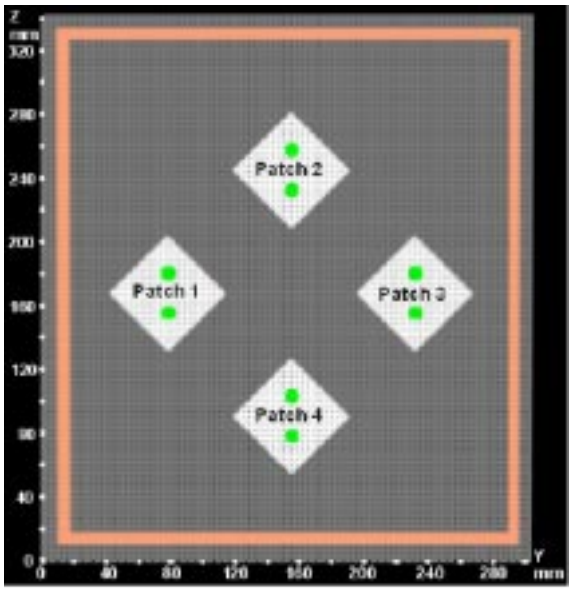


Note that the patches have been designated by numbers 1 through 4 in a clockwise direction beginning with the most left patch. Figure 9.4 illustrates a section in the x-z plane of the mesh through the active patches, associated stripline circuitry of the antenna and the sides of the Luran S plastic radome with the Kuster head in a position for exposure.

*Figure 9.4*

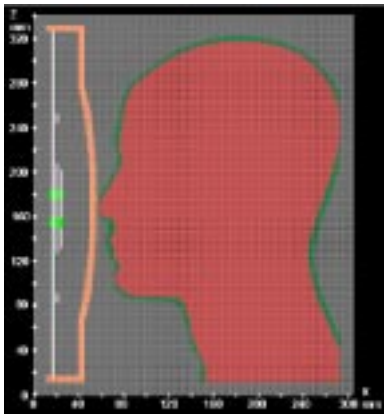

The spacing between the adjacent faces of the 1 mm thick ground plane and the 1 mm thick RF stripline circuitry is 4 mm and that between

adjacent faces of the stripline circuitry and the square upper patches is also 4 mm. The antenna used in most of these studies did not include the radome since the dielectric properties of the Luran S plastic material were not available over most of the time of the study. However, the dielectric constant of 2.97 and the loss tangent of 0.0154 (conductivity of 0.006 S/m) at 2.357 GHz did become available prior to the conclusion of the study. Rather than repeat all of the calculations it was decided to determine the effect of the presence of the radome on the “worst case” calculated SAR distributions. This case corresponded to exposure of the Kuster head model with the tip of the nose centered over patch No. 1 (the left most patch at the face of the antenna). At first a simple flat sheet of the Luran S material 4 mm thick was used to simulate the radome. Since it was found to significantly lower the peak SAR by a factor of 1.5 to 2.0 it was decided to more closely model the radome as close as possible to its true shape within the existing FDTD model space. This was accomplished by first using the GUI of the FDTD code to model a square radome including a flat rectangular edge surrounding a combination of a flat disk at the center of the radome with spherical sides sloping down to the rectangular edge. A FORTRAN computer code was then written to shape the square radome into a rectangular shape of proper dimensions with the required ellipsoidal shape of proper dimensions at the central region of the radome as shown in Figure 9.4 in the x-z plane. Figure 9.5 provides a similar graph of the model in the x-y plane at z = 165.

*Figure 9.5*

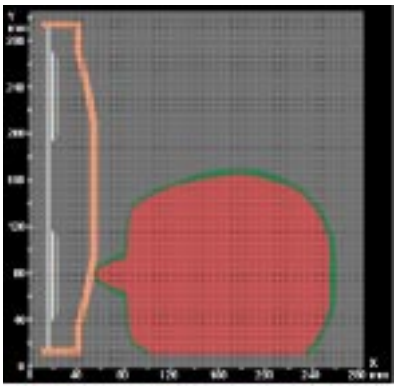

The nose of the head models was always placed at the position where it would contact the outer surface of the radome (head facing surface) whether the radome was present or not. It was found that with the more

realistic shape radome attached to the antenna the calculated peak SAR was 1.9 dB lower than the calculated value obtained without the presence of the radome. The calculated 1 gram average SAR was found to be 0.86 dB lower when the radome was attached.

### 9.4.2 Kuster Homogeneous Head Model

The FDTD model of the Kuster experimental phantom head derived from a file containing data from MRI scans of the SPEAG head and upper torso human model used in the previous study was also used in this study. The nose of the model was oriented with the tip in contact with the antenna radome at the center of patch No 1 since that patch was found to provide the highest values of SAR distributions. The latter proved to result in the highest SAR in the exposed nose of the model. A dielectric constant of 2.54 was assigned to the Plexiglas shell and the relative permittivity and conductivity of the liquid used to simulate the brain tissue in the experimental model were assigned values of 39.37 and 1.717 S/m, respectively. These are the values published in a draft of recommended practice by IEEE Standards Board, SCC34 on certification of wireless phone safety as appropriate for use as an equivalent head tissue for phantom heads at 2357 MHz.

#### 9.4.2.1 Nose of Model Centered Over Geometric Center of Patch Array

Figure 9.6 illustrates the x-z section through the tip of the nose of the head and shoulders model positioned at the center of the array of antenna patches in the FDTD mesh.

*Figure 9.6*

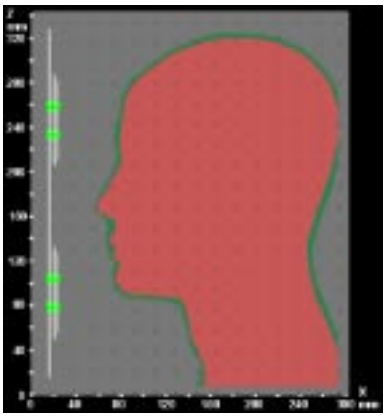

The tip of the nose was assumed to be located so it would contact the outer surface of the radome if it were present. Since the radome was spaced further from the antenna and was constructed of thicker material than that for the previous analysis, the mesh space had to be expanded from 270 mm to 285 mm in the x direction. In the previous analysis part of the back of the head and shoulders of the model had to be truncated to keep the size of the FDTD space within the 1 Gbyte RAM limit. With the expansion of the mesh it was found that 1 Gbyte of RAM was insufficient to contain the mesh so the RAM had to be expanded to 2 Gbytes. With the expansion it was found that the Windows 98 operating system would no longer boot up so it was replaced with the Windows 2000 operating system. Figure 9.7 illustrates the x-y section of the model at the slice through the nose of the model where the peak SAR was observed.

*Figure 9.7*

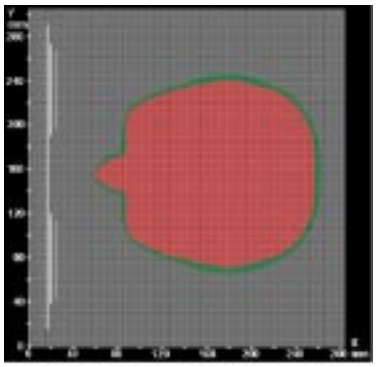

#### 9.4.2.2 Nose of Model Centered Over Geometric Center of Patches 1 Through 4

Figure 9.4 and Figure 9.5 discussed previously illustrated the position of the Kuster head model exposed with the tip of the nose centered over patch 1. Figure 9.8 illustrates the x-z section through the tip of the nose of the head and shoulders model at slice 156 of the FDTD mesh at the center of patch 2 (the upper patch).

*Figure 9.8*

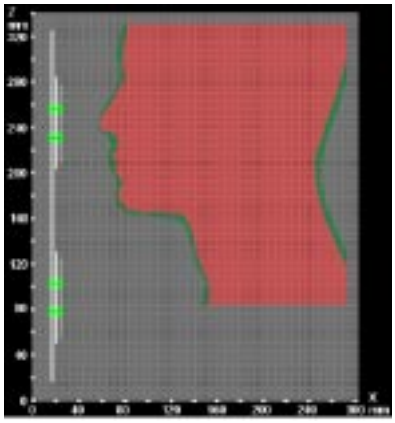

Figure 9.9 illustrates the x-y section of the model at slice through the nose of the model where the maximum peak SAR was observed.

*Figure 9.9*

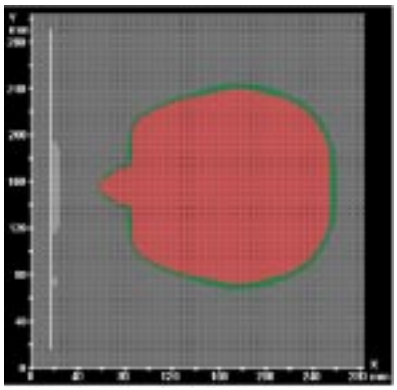

Figure 9.10 and Figure 9.11 illustrate the respective views in the x-z and x-y sections with placement of the model in front of patch 4 (the lowest patch).

*Figure 9.10*

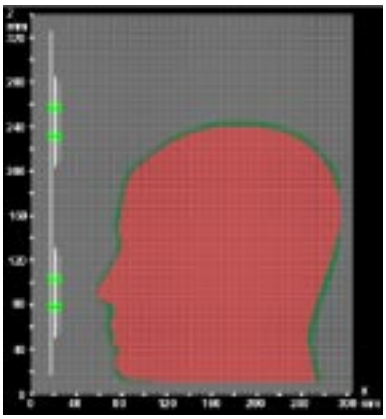

*Figure 9.11*

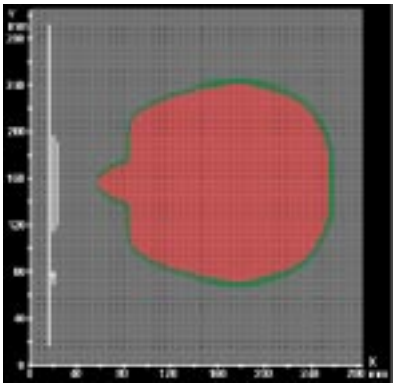

No exposures were made for the model nose centered over patch 3 (the most right patch) since by symmetry it should produce the same results as obtained for the model nose centered at patch 1. Actually the fields were higher at patch 4 than patch 3 so exposures to patch 4 corresponded to a “worst case”.

### 9.4.3 REMCOM Head and Shoulders Model

The REMCOM XFDTD head model used in this study was the same as used previously. It is based on the “visible man” model derived from a project under the direction of the National Library of Medicine. The original file is based on taking thin slices successively along a plane perpendicular to the long axis of a frozen deceased human and

successively photographing the freshly cut surfaces of the remaining portion of the body. Information on the project is available on the Internet at http://www.nnlm.nlm.nih.gov/sar/curr/95n6/nlmunvei.html. REMCOM modified the file by thinning out the slices and adding the dielectric properties for each of the major tissues, resulting in a three dimensional FDTD meshed model of approximately 861500 cells (voxels) of 5x5x5 mm in size. A head and shoulders model meshed to a voxel size of 3x3x3 mm was also supplied. The cell size of the latter model used in this analysis was too large to obtain the desired SAR spatial resolution of 1-mm so a command feature of the XFDTD was used to decrease the cell size down by a factor of three yielding a head and shoulders model that was used to replace the SPEAG head model in the 285x306x342, 1-mm voxel space containing the antenna. Of course the reduction doesn't increase the resolution of the tissue structure but does improve the spatial resolution of the calculated SAR distribution and allows the model to occupy the same 1-mm mesh containing the antenna. Gabriel's (1996) equations were used to determine the respective relative permittivities and the conductivities at 2.357 GHz for bone, 18.7 and 0.773 S/m; brain (white matter), 49.1 and 1.74 S/m; cartilage, 39.0 and 1.68 S/m; eye, 52.8, 1.97 S/m; muscle, 54.5, 1.81 S/m; and skin, 38.1, 1.42 S/m. It was assumed that the change in dielectric properties from 1.92 GHz to 1.8675 GHz was negligible. Figure 9.12 illustrates section of the model in the x-z plane at x = 80 (sagittal plane, the slice through the center of the head).

*Figure 9.12*

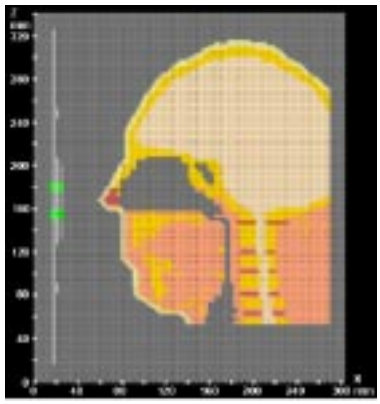

Figure 9.13 illustrates the section of the model in the x-y plane at z = 171.

*Figure 9.13*

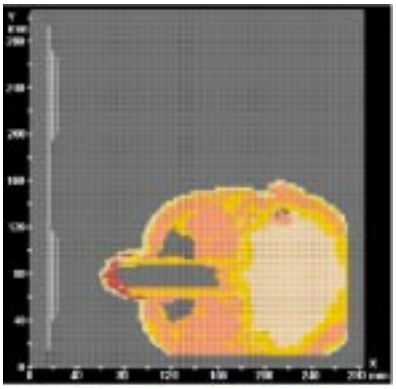

## 9.5 FDTD Calculation and Measurements of SAR in Kuster Head and Shoulders Homogeneous Model

FDTD calculations were made of the peak and 1-gram average of the SARs in the Kuster homogeneous head model (described in Section 9.4.2) exposed to the AT&T RU Cushcraft antenna. Graphical SAR data files and plots calculated throughout the entire head model were scaled for an input power of 158.5 mW to the antenna which corresponds to a far-field effective radiated power of 4.00 watts from the antenna with no models present.

The safe exposure standards in the United States for the public or uncontrolled environment including the FCC MPLs are based on limiting the maximum SAR as averaged over any gram of tissue in the shape of a cube to 1.6 W/kg and the SAR as averaged over the whole body to 0.08 W/kg. Thus the FDTD calculated SAR distribution data must be converted some way to reflect the average over any gram of tissue in the shape of a cube. At the time of the previous RU antenna analysis to the present there was no standardization on how this averaging process should be done to account for the irregular shape of tissue boundaries such as encountered at the ears, nose, mouth, etc. If the averaging routine maintains the 1-gram cube entirely within the tissue boundaries so that a flat face of the cube cannot emerge outside of the tissue boundaries, the averaging process may miss regions of high SAR which commonly occur at the surface or at

locations where there are sharp curves of the tissue surface. This will result in a lower average SAR than would be the case if the surfaces of the cube were allowed to extend beyond the tissue boundaries in order not to miss any tissue with high SAR near an irregular boundary. The latter could include a large amount of air in the averaging volume, requiring the cube to become larger to encompass the required gram of tissue thereby allowing more surface tissue with the higher SARs to weight the averaging process. In using the XFDTD version 4.04 software in the previous study, the FDTD averaging routine considered a cube of space centered at each FDTD cell within the tissue. The cube was then allowed to expand until a gram of tissue was contained within its boundaries. When 1 gram of tissue (to within 1% accuracy) was contained in the cube the SAR was averaged over the entire cube and the average value was assigned to the cell at the center of the cube. It should be realized that this could lead to pessimistically higher values of SAR at distances from the tissue surface that are shorter than the dimension of the averaging cube. In using the new XFDTD version 5.05 code in this analysis the routine is less pessimistic by imposing an additional condition that the face of the averaging cube not be extended into the air anymore than necessary to enclose all of the tissue below the outermost point of the tissue boundary. However with this modification it is possible that not all voxels are included in the averaging process. This caveat is emphasized in the following statement in the XFDTD v5.05 operating manual

“The sample cube must meet some conditions to be considered valid. The cube may contain some non-tissue cells, but some checks are performed on the distribution of the non-tissue cells. A valid cube will not contain an entire side or corner of non-tissue cells. If the cube is found to be invalid, the averaging for the center cell will stop and move on to the next cell. It is possible (and probable) that some cells will not be the center of an average. However, these cells will often be part of an average cube for an adjacent cell.”

Fortunately new standards for the averaging process have been agreed upon and approved by the IEEE Standards Board, SCC34 on certification of wireless phone safety. The new standard which will become part of the new exposure standard will insure (a) the averaging cube will wherever possible be kept within the tissue boundaries and will not extend out to the air and (b) perform tests to confirm that all voxels have been included in the averaging and (c) if any voxels have been excluded, allow whatever air is necessary to be contained in the

averaging cube to allow the voxels to be included in the averaging process.

### 9.5.1 Orientation with Tip of Nose in Contact with Radome at Center of Four Patch Array

Figure 9.14 illustrates the FDTD derived SAR distribution in the x-z plane through the center of the head exposed with the nose in contact with the radome over the geometric center of the four patch array.

*Figure 9.14*

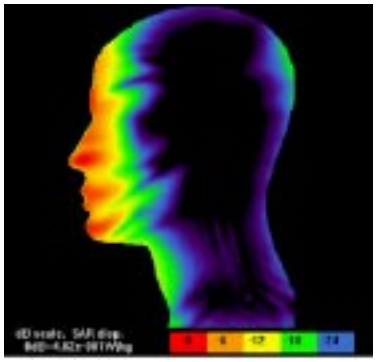

The SAR distributions as averaged over each 1 mm cubical cell or voxel, calculated by the FDTD program are depicted as a color graphs with each color representing a 6 dB range of SAR values. The maximum SAR corresponding to the 0-dB reference is shown below each graph. Figure 9.15 illustrates the SAR distribution in the horizontal xy plane where maximum SAR was observed.

*Figure 9.15*

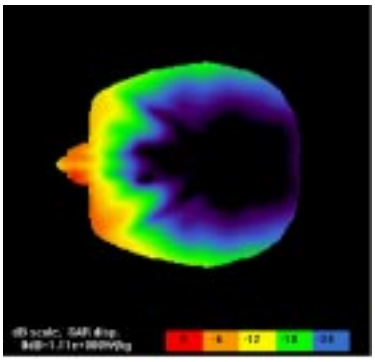

Figure 9.16 illustrates a color plot of the maximum 1 gram averaged SAR distribution in the xy plane.

*Figure 9.16*

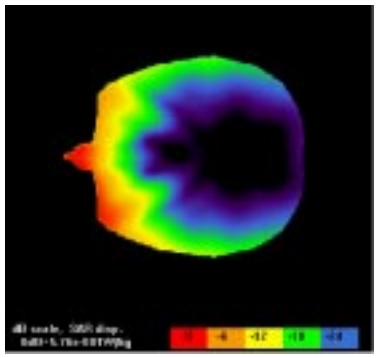

### 9.5.2 Orientation with Tip of Nose Centered over Path No. 1 (no radome attached)

Figure 3.4 illustrates the FDTD derived SAR distribution in the x-z plane at y = 80 through the center of the head exposed with tip of nose centered over patch No. 1 and in contact with position where outer surface of radome would normally be placed. Figure 9.17 illustrates the SAR distribution in the horizontal xy plane at z = 165 where maximum SAR was observed.

*Figure 9.17*

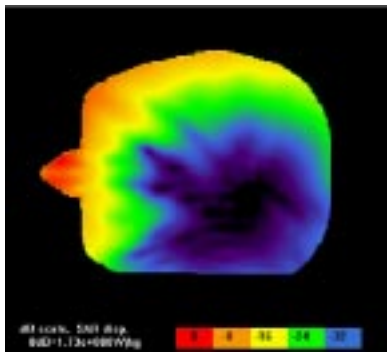

Figure 9.18 illustrates a color plot of the maximum 1 gram averaged SAR distribution in the xy plane at z = 168.

*Figure 9.18*

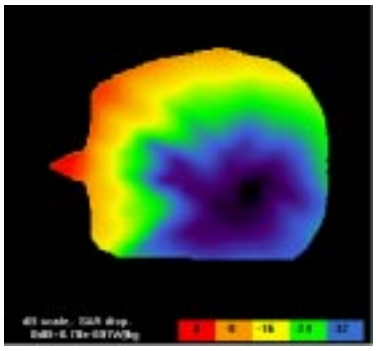

### 9.5.3 Orientation with Tip of Nose Centered over Path No. 1 (radome attached)

Figure 9.19 illustrates the FDTD derived SAR distribution in the x-z plane through the center of the head exposed with the nose in contact with the radome over the geometric center of patch No. 1.

*Figure 9.19*

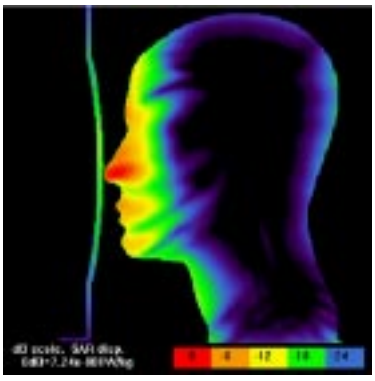

Figure 9.20 illustrates the SAR distribution in the horizontal xy plane at z = 165 where maximum SAR was observed.

*Figure 9.20*

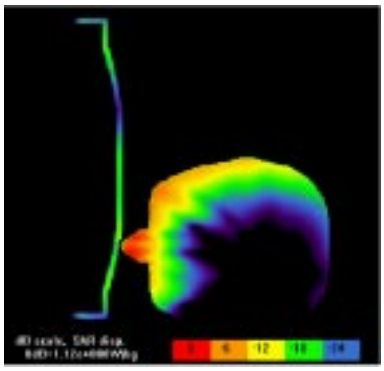

Figure 9.21 illustrates a color plot of the maximum 1 gram averaged SAR distribution in the xy plane at z = 168.

*Figure 9.21*

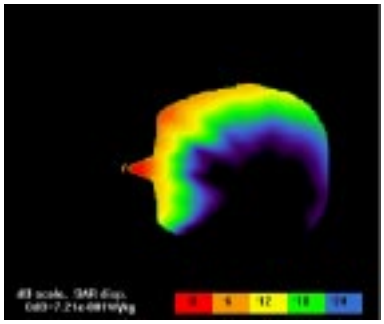

### 9.5.4 Orientation with Tip of Nose Centered over Patch No. 2 (no radome attached)

Figure 9.22 illustrates the FDTD derived SAR distribution in the x-z plane at y = 156 through the center of the head exposed with tip of nose centered over patch No. 2 and in contact with position where outer surface of radome would normally be placed.

*Figure 9.22*

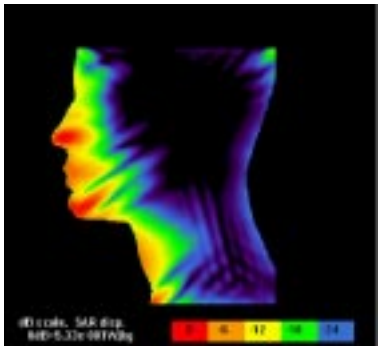

Figure 9.23 illustrates the SAR distribution in the horizontal xy plane at z = 242 where maximum SAR was observed.

*Figure 9.23*

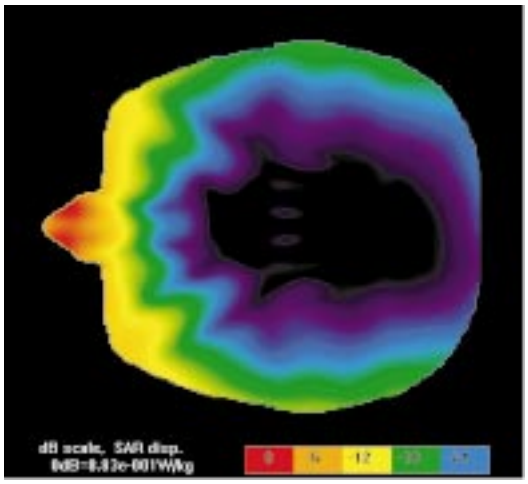

Figure 9.24 illustrates a color plot of the maximum 1 gram averaged SAR distribution in the xy plane at z = 242.

*Figure 9.24*

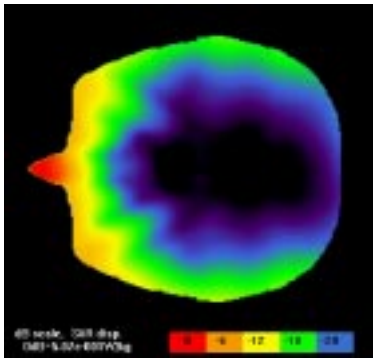

### 9.5.5 Orientation with Tip of Nose Centered over Patch No. 4 (no radome attached)

Figure 9.25 illustrates the FDTD derived SAR distribution in the x-z plane at y = 156 through the center of the head exposed with tip of nose centered over patch No. 2 and in contact with position where outer surface of radome would normally be placed.

*Figure 9.25*

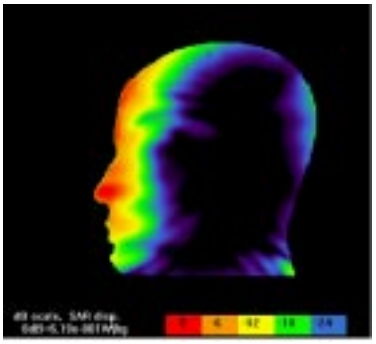

Figure 9.26 illustrates the SAR distribution in the horizontal xy plane at z = 146 where maximum SAR was observed.

*Figure 9.26*

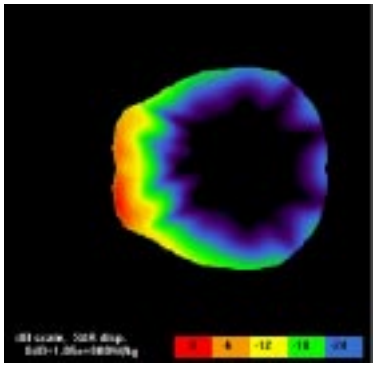

Figure 9.27 illustrates a color plot of the maximum 1 gram averaged SAR distribution in the xy plane at z = 92.

*Figure 9.27*

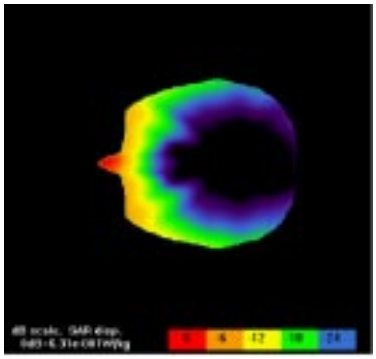

## 9.6 FDTD Calculation of SAR in REMCOM Head and Shoulders Inhomogeneous Model (no radome attached)

FDTD calculations were made of the peak and 1-gram average of the SARs in the REMCOM inhomogeneous head model exposed to the AT&T RU antenna. The head was exposed with the face toward the antenna with the tip of nose centered over patch No. 1 and in contact with position where outer surface of radome would normally be placed. Graphical SAR data files and plots calculated throughout the entire head model was scaled to correspond to an input power of 158.5 mW to the antenna. Figure 9.28 illustrates the SAR distribution in x-z plane at y = 80 through the center of the head.

*Figure 9.28*

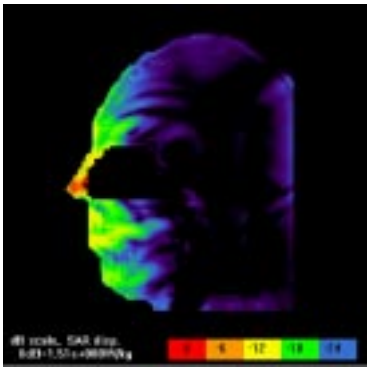

Figure 9.29 illustrates the SAR distribution in the horizontal xy plane at z = 171, the slice where maximum SAR was observed.

*Figure 9.29*

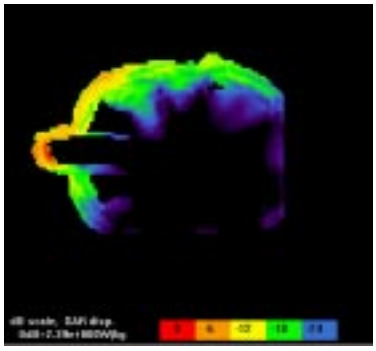

Figure 9.30 illustrates a color plot of the maximum 1 gram averaged SAR distribution in the xy plane at z = 173.

*Figure 9.30*

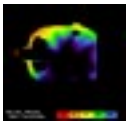

Peak and 1 gram average SARs for various computer tissue phantoms consisting of homogeneous and inhomogeneous human head models exposed to the AT&T RU Cushcraft antenna were calculated. The results in Table 1.0 show that the worst case scenario is exposure of the head with the tip of nose centered over patch No. 2 and in a position where outer surface of the radome would normally be placed. This case results in an exposure of 2.61 dB below the FCC MPL of 1.6 W/kg when the antenna is operating with 158.5 mW input corresponding to an e.i.r.p. of 4 watts. It is highly unlikely that such an exposure would last for the 30 minute averaging time specified by the FCC and most likely would only be momentary if it ever occurred in practice. For example an 18-second exposure under these conditions would result in SARs 20 dB below the FCC MPL. As expected the exposure of the more life-like inhomogeneous head model results in SARs lower than obtained from the worst case homogeneous models. The table also shows comparisons of calculated SAR levels with FCC MPLs for e.i.r.p. levels of 2 watts and 3 watts. For example a 50% duty cycle would result in the worst case SAR of being 5.61 db below the FCC MPL.